Lasers in Manufacturing Conference 2019

Applied machine learning for predicting the weld seam geometry based on the example of laser-assisted metal-plastic joining

Klaus Schricker[a]*, Marcus Glaser[a], Jean Pierre Bergmann[a]

[a]*Technische Universität Ilmenau, Production Technology Group, Mittelstand 4.0-Kompetenzzentrum Ilmenau, Gustav-Kirchhoff-Platz 2, 98693 Ilmenau, Germany*

Abstract

In this paper, supervised neural networks and support vector machines are used to predict the weld seam geometry in laser-assisted metal-plastic joints. The informative value was maximized by generalizing the training data to geometrical properties, material data and process parameters. The meaningfulness is determined by 10-fold cross-validation during the training process and different amounts of training data. Finally, referencing investigations on novel parameters were carried out to evaluate the informative value of the applied machine learning methods.

Keywords: Joining, System Technology and Process Control, Fundamentals and Process Simulation, Machine Learning, Neural Nets

1. Introduction and state of the art

Digitalization is gaining increasing importance in mechanical engineering and the closely related field of joining and welding technology. In addition to the networking of production facilities, digital services in the business model or the use of digital twins of products and facilities, Artificial Intelligence (AI) is a central issue. Especially for complex tasks in joining technology, AI techniques, e. g. machine learning, can be used to estimate process parameters for new materials, modified alloy compositions or sheet thicknesses.

* Corresponding author. Tel.: +49-3677-69-3808; fax: +49-3677-69-1660
E-mail address: klaus.schricker@tu-ilmenau.de

Machine learning addresses the use of algorithms that improve automatically through experience (Mitchell, 2006). In recent years, several researchers have applied machine-learning methods for modeling mutual influence between process parameters in different laser manufacturing applications. Examples are given for process control (Günther et al., 2016, Stavridis et al., 2018) or quality assurance (Wasmer et al., 2018, Knaak et al., 2018, Yuan et al., 2018). In each case, process data were used for training the machine learning technologies, e. g. acoustic signals, photodiodes, image data or x-ray data. Other approaches are focused on the investigation of combining machine-learning applications with numerical simulations of laser welding (Akbari et al., 2016). It should be noted, that a trained artificial intelligence produces the information within seconds in contrast to numerical simulation while licenses or material data are no mandatory requirement. Further investigations deal with the challenge to establish a valid relationship model between input and output parameters in laser-based processing of thermoplastics (Acherjee et al., 2011). In addition, investigations have been carried out regarding the combination of different machine learning methods like neural nets and genetic algorithms (Liu et al., 2018) or Support Vector Regression (SVR, Petković, 2017) to optimize laser process parameters or predict geometry characteristics.

Especially supervised feed forward network structures based on backpropagation learning approaches are well established (Balasubramanian et al., 2010, Sathiya et al., 2012, Nikolić et al., 2016, Jacques and Abderrazak, 2018). These types of artificial neural networks are powerful tools as they are suitable for problems, which are not amenable to exact analytical solutions. Large sets of parameter patterns can be stored as memories for the system, which can be recalled later. Furthermore, these techniques can reduce the dimensionality of the original data set to a simpler representation with fewer dimensions. The literature review demonstrates that the non-linear interrelations between input and output parameters, as they occur in laser welding processes, can be approximated.

A novel application regarding laser welding is the prediction of weld seam geometries in order to provide information for new engineering constructions and components. In laser-assisted polymer-metal joining, the laser beam is absorbed at the metal surface and heat conduction across the interface between both materials leads to melting of the polymer (Fig. 1a, b). The surface of the metallic joining partner roughened by previous processes has nano- or micro-scale structures which can be wetted or filled by the molten polymer (Al-Sayyad et al., 2018, Heckert and Zaeh, 2014, Fig. 1b). Solidification creates a solid connection between the two materials when the laser beam is turned off after a certain time (t_L, Fig. 1c). The resulting joining zone is mainly characterized by the melting layer in the thermoplastic material. On the one hand, the diameter of the melting zone and the temperature distribution influence the bonding surface between the two materials (Schricker and Bergmann, 2019). On the other hand, the material thickness of the plastic component is limited, e. g. for plastic carriers in household appliances. For this reason, the melt layer thickness must be considered as a predominant factor for the evaluation of process quality, since its size is not allowed to weaken the component structure. A further description of the melting layer and its effects on the joint is given in Schricker, 2018.

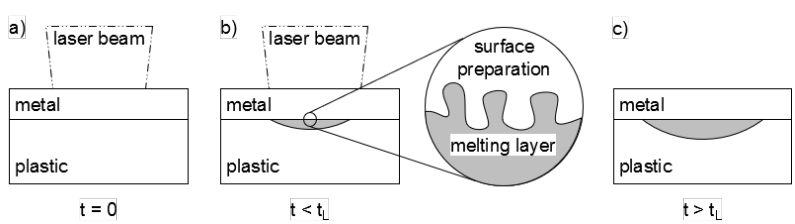

Fig. 1. (a) Process start with metal and polymer in contact; (b) formation of the melting layer during; (c) joint after solidification

The implemented approach presented in this paper is based on the idea of combined application of process parameters and material specific parameters to an artificial neural network-based model with the goal to predict the geometry of welds in thermal joining of metals and polymers. Next to specific process parameters like laser power or welding time material-specific qualities and metallurgical properties of the joining parts like melting temperature, enthalpy or thickness are considered. Both experimental results as well as simulation data is used for training and validation of the applied machine learning technique while the quality of the welding joints is determined based on the geometrical parameter melting layer thickness.

2. Methodical approach and experimental realization

2.1. Experimental setup and materials

The experiments were carried out using a diode laser (Laserline LDM 3000, $\lambda = 980$ nm) with a focal diameter of 5.3 mm and an applied beam power P_L of 1,000 W. The processing optic and the clamping device were mounted on a three-axis portal. In terms of fundamental research, spot joints were manufactured in heat conduction joining. The overlap had a width of 100 mm and a length of 75 mm. Joining times (t_L) from 1 s up to 10 s were investigated. The distance between the clamping jaws was fixed at 50 mm to avoid heat accumulation. Aluminum EN AW 6082 with a thickness of 1.5 mm was used as metal joining partner. The surface of the metal sheet was used in the as-delivered state as the focus of the investigations is on the geometry of the melt zone and not on achievable strengths. Polyamide 6.6 with a thickness of 5 mm was chosen as polymeric joining partner in the main experiments. Additionally, polyamide 6 and polypropylene were used in the preliminary investigations. The thickness fulfills the requirement of the semi-infinite body in order to avoid heat accumulation within the thermoplastic material. Both joining partners were cleaned with isopropyl before the experiment. The experimental setup is shown in Fig. 2a.

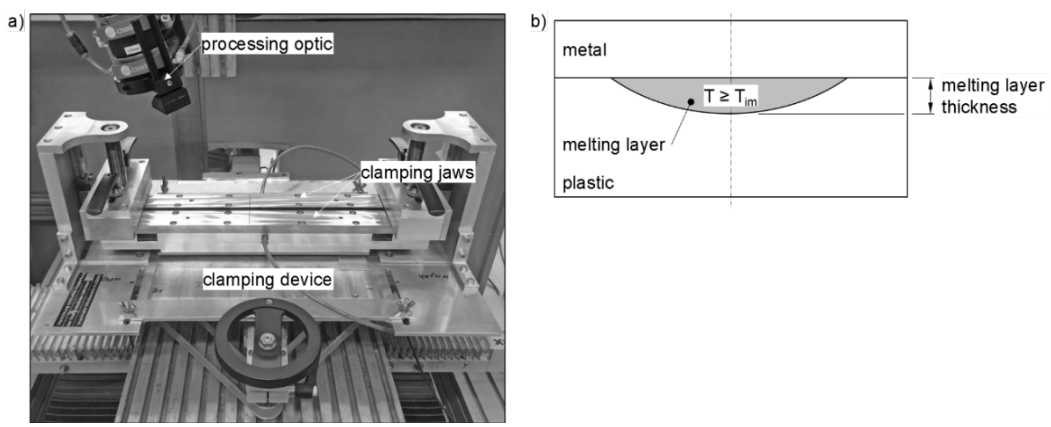

Fig. 2. (a) experimental setup; (b) melting layer thickness ($t_{melting\ layer}$) of the spot joint

Based on the joining process, a melting layer forms in the thermoplastic joining partner. This area depends on the temperature distribution within both joining partners and shows different morphological zones (see also Schricker et al., 2015). The characteristic temperatures were described in Schricker and Bergmann, 2018 and Schricker, 2018. In the present case, only the starting temperature of the melting interval T_{im} ($T_{im,\ PA\ 6.6} \approx 235$ °C, $T_{im,\ PA\ 6} \approx 191$ °C, $T_{im,\ PP} \approx 126$ °C) is considered, as it is responsible for the maximum extent of melting layer thickness respectively diameter. In order to describe the geometry of the weld seam, the melt zone thickness is used at this point (see Fig. 2b).

2.2. Numerical simulation

A thermal model was used to determine the temperature distribution in both joining partners and thus also the melt zone thickness. The simulations were carried out using Comsol Multiphysics 5.2a. The characteristic temperature T_{im} was determined by differential scanning calorimetry. The material properties density, heat conductivity and specific heat were considered temperature dependent. The thermal analysis, the geometry and the boundary conditions are described in detail in Schricker and Bergmann, 2018 as well as in Schricker, 2018.

Based on the valid numerical simulation, different laser beam powers (P_L) and metal sheet thicknesses (t_M) were examined to provide further data to train the machine learning algorithms.

2.3. Application of machine learning

The presented investigations were implemented using a feed forward multilayer neural network. Besides necessary input and output layer, the network is constructed with two additional hidden layers. Following the approach of supervised learning, the parallel processing network is trained with backpropagation for determining the complex relationships between input variables and to generate an associated output in response. Therefore, the initial weights and biases will be iteratively adjusted to increase the network performance and minimize the occurring mapping error (i.e. the residual mean square error, MSE).

Based on preliminary testing with available experimental data, a valid and efficiently network structure was derived. Therefore, different number of models were evaluated concerning their prediction performance is based on the principle of reducing statistical characteristics like sum of squared errors (SSE), the residual root mean square error (RMSE) as well as the coefficient of determination (R^2).

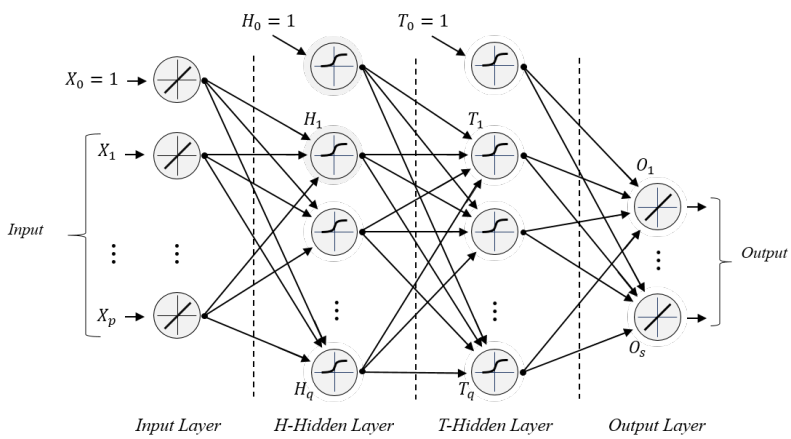

Fig. 3. Schematic structure of the applied neural network structure

As shown in the schematic in Fig. 3, the network consists of neurons, which are completely connected to each following neuron of the adjacent layer. The output of each layer will be defined by the sum of input signals and their related weights, the threshold value as well as the defined activation function. Tan-sigmoid functions were applied in the hidden layers and transfer functions in the input and output layer. The output of the network therefore results as it is shown in Eq. 1, where f_{act} is the activation function for the considered layer and α, β, γ are the specific weights with regard to the preceding layer. The network performance is significantly influenced by the number of hidden layers and neurons in these hidden layers.

In this paper the used network structure consists of 12 neurons in the input and first hidden layer, as well as 6 neurons in the second hidden layer and one output neuron in the output layer. This network architecture turned out as especially powerful and less prone to errors dealing with the provided experimental data and simulated data sets as a result of preliminary tests.

$$NET_{out} = f_{act}^{O-L}\left\{\sum_{k=0}^{r}\gamma_{kl} * f_{act}^{T-L}\left[\sum_{m=0}^{q}\beta_{mk} * f_{act}^{H-L}\left(\sum_{n=0}^{p}\alpha_{nm}X_n\right)\right]\right\} \quad (1)$$

The gained results were compared to a support vector regression (SVR). Thereby a nonlinear mapping of data into defined feature spaces is used in which a linear separation becomes possible. The application of a so-called kernel function is required to map the data to the higher dimensional feature space. For this investigations, a radial basis kernel function depicted in Eq. 2 is used.

$$k(\vec{x}, \vec{x}') = exp(-|\vec{x} - \vec{x}'|^2/2\sigma^2) \quad (2)$$

The results were evaluated based on the statistical indicators of mean-absolute error (MAE), root-mean-square error (RMSE) and coefficient of determination (R^2) (see Eq. 3, Eq. 4 and Eq. 5) where ϕ_p and ϕ_q are the predicted and original values over the total number of considered data points n.

$$MAE = \frac{1}{n}\sum_{i=1}^{n}\left|\phi_p - \phi_q\right| \quad (3)$$

$$RMSE = \sqrt{MSE} = \sqrt{\frac{1}{n}\sum_{i=1}^{n}\left(\phi_p - \phi_q\right)^2} \quad (4)$$

$$R^2 = \frac{\left[\sum_{i=1}^{n}\left(\phi_q - \overline{\phi_q}\right) * \left(\phi_p - \overline{\phi_p}\right)\right]^2}{\sum_{i=1}^{n}\left(\phi_q - \overline{\phi_q}\right) * \sum_{i=1}^{n}\left(\phi_p - \overline{\phi_p}\right)} \quad (5)$$

3. Results and Discussion

3.1. Melting layer in thermal joining

The melting layer thickness over joining time t_L is given in Fig. 3 for the experiment and the numerical simulation. The melting layer thickness increases from approx. 90 µm after a joining time of 1 s to approx. 530 µm after a joining time of 10 s. The course of simulation and experiment follows the same characteristics of an exponential function. The relationship is correctly represented by the simulation and the deviation of the melting layer thickness between simulation and experiment is mainly within the empirical standard deviation. A maximum deviation in melting layer thickness is 9.9 % at a joining time of 1 s which corresponds

to an absolute deviation of 8.8 µm. The diameter of the melting layer also corresponds very well to the experiment, as already explained in Schricker and Bergmann, 2018.

The high agreement between simulation and experiment allows to provide further data for the training of the AI by numerical simulation, e. g. by varying the material thickness (t_M) or the laser beam power (P_L).

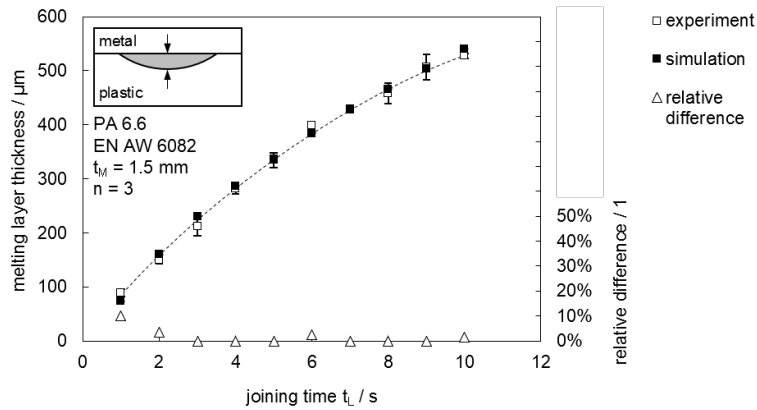

Fig. 4. Comparison of experiment and numerical simulation for melting layer thickness (P_L = 1.000 W)

3.2. Investigations on different machine learning algorithms and prediction of the melting layer thickness

The initial test aims at the performance of a feed forward multilayer neural network applied to the available experimental data. In this database the process parameters as well as the used sheet metal remain constant (EN AW 6082), while the used material parameters for plastic components (PA6, PA6.6, PP) vary. Different joining times in the range from 1 s up to 10 s are considered. The data sets were taken from experimental investigations only.

The available dataset consists of 84 instances and 12 attributes. Eight instances are randomly selected for future testing while the rest is used for training. The 10-fold cross-validation is used to train the network, while each fold takes 0.82 s computing time in single core mode for the defined maximum number of 2,000 iterations for the backpropagation cycle. After a training and validation time of about 10 s, the network is trained and can be applied to the test set. The results require a computational time of less than 0.01 s. The training and testing data are also applied to SVR in comparison. The results are illustrated in Fig. 5 and Tab. 1 for MLP (a) and SVR (b). The histogram plots as well as their related frequency tables are given over the error class margin, which expresses the deviation from the target melt layer thickness. The results demonstrate, that the neural net reaches a lower error compared to the applied SVR-method. In 90 % of the cases, the error is less than 40 µm in a total range of target attribute values between 0 up to 850 µm. The SVR shows a lower accuracy since only 76 % of the predicted values have an error of equal or less than 40 µm. In three cases, the error increases to over 100 µm, which could not be determined with MLP. The performance of both procedures at the testing data is also considered in more detail. The predicted deviation to the original value (Fig. 5c) as well as the actual error (Fig. 5d) are indicated. These diagrams illustrate that the neural net as well as the SVR method predicts the original test values well, whereby the MLP shows a better performance, which becomes apparent in conjunction with the values for MAE and RMSE in Tab. 1. Moreover , in most cases the neural net prediction seems to be lower than the real values. This cannot be observed for the results made by the SVR.

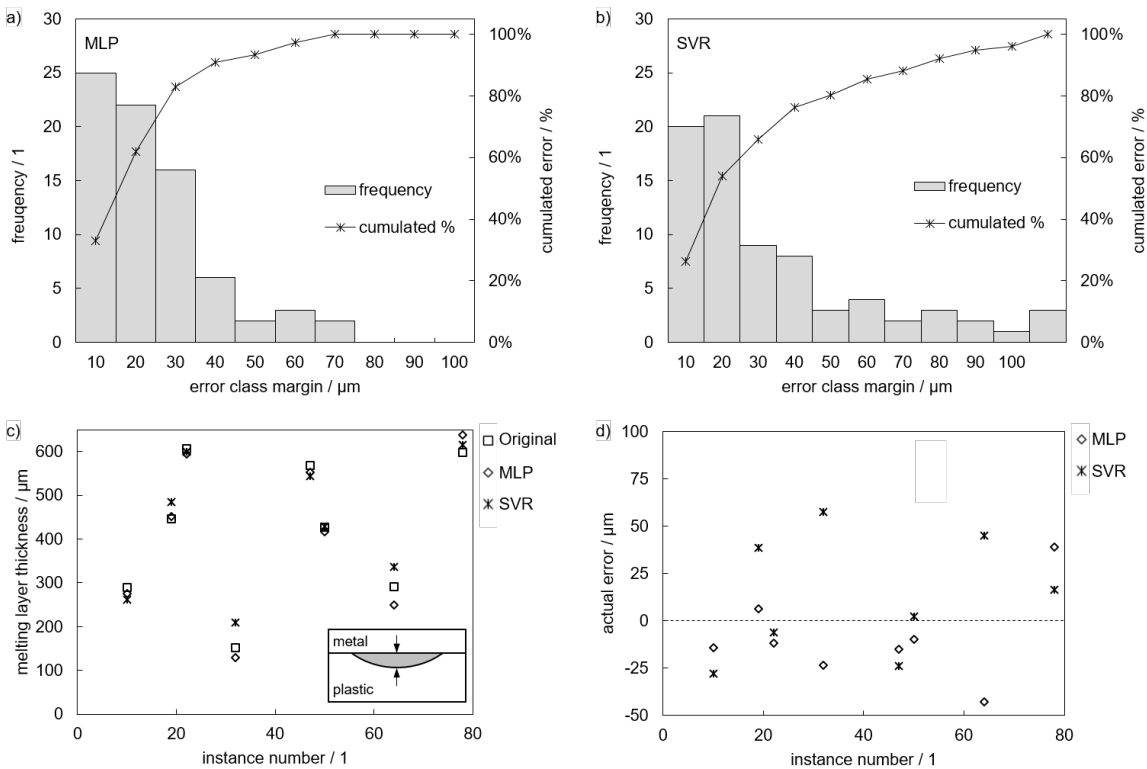

Fig. 5. Training histogram for MLP (a) and SVR (b); deviation of the MLP and SVR result to the original value (c); actual error of MLP and SVR result (d)

Table 1. Statistical indicators for training and test of the MLP and SVR

Machine learning system	Data set	R^2 / 1	MAE / µm	RMSE / µm
MLP	Training	0.9923	18.6617	23.8066
	Test	0.9944	20.3154	24.0014
SVR	Training	0.9744	29.9569	43.6112
	Test	0.9833	27.2241	32.5440

3.3. Prediction of the melting layer thickness

In the following chapter, the experimental data were replaced by computationally generated data sets and calculated based on the shown MLP. Therefore, a valid model is available as shown in chapter 3.1 which allows the supplement of several data sets depending on process variables, material data and geometrical parameters. Based on this simulation, a large number of consistent and accurate data of the melting layer can be provided. A further advantage is the short computational times of each data point of approx. one minute at four cores. The next step is to evaluate the neural network performance in the task of interpolation and extrapolation of specific prediction points based on a strictly simulated training set. Therefore, the training data set consists of 30 instances with variations in the attribute of sheet metal thickness (t_M = 1.5 mm, 2.0 mm, 2.5 mm). The introduced laser power (P_L = 1,000 W) as well as the applied

thermoplastic material (PA 6.6) remains constant. The maximum number of training iterations at each cross-validation fold is raised slightly up to 5,000. The training time per fold is around 0.69 s as a consequence of the low number of training instances. After a total time of 7 s, the network is trained and can be used for testing. The applied test data consists of two data points for sheet metal thickness of $t_M = 1.0$ mm (extrapolation) and $t_M = 1.7$ mm (interpolation) which were not part of the training data. The results are shown in Fig. 6. Based on the limited amount of training data, the MLP shows a high level of agreement for the interpolation at $t_M = 1.7$ mm with a deviation below 1 %. For the approximation of the sheet thickness ($t_M = 1.0$ mm), the deviation increases to approx. 7 % which represents an actual error of 39 µm. The computed data point by the MLP is pulled towards the lower sheet thicknesses used in the training of the neural net. Nevertheless, a reasonable forecast is achieved.

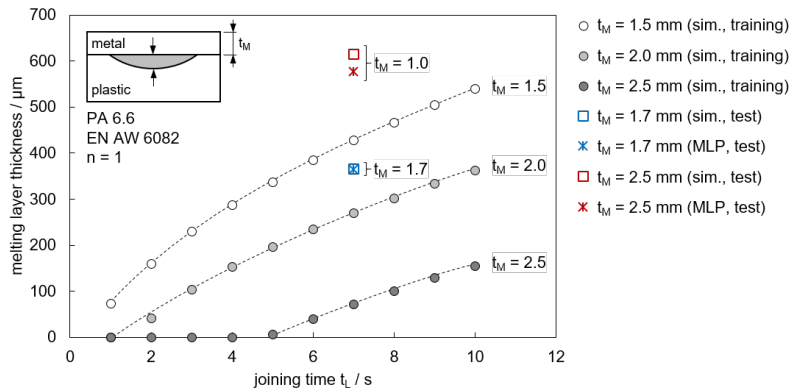

Fig. 6. Data sets for training, interpolation and extrapolation for the MLP (P_L = 1,000 W, t_M = var.)

This is followed by an extension of simulated training data for different laser beam powers as well as varied metal sheet thicknesses. The prediction of different parameters is given in Fig. 7 for an extrapolated joining time of 12 s based on different parameters. The results differ greatly from each other. For the interpolation of the large material thickness ($t_M = 2.3$ mm), few training points are available resulting in a large error. For the lower material thicknesses ($t_M = 1.7$ mm) the predictions are much more precise.

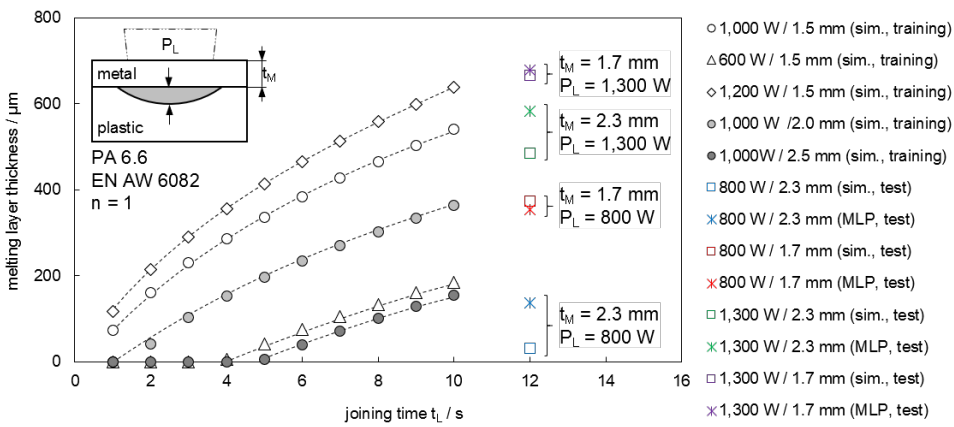

Fig. 7. Data sets for training and extrapolation for the MLP (P_L = var., t_M = var.)

From this it can be concluded that the quality of the results depends strongly on the training data and their volume. The present attempt to achieve sufficient results on the basis of less training data is nevertheless positive, since the results achieved in Fig. 7 could be represented on the basis of only 50 training sets.

3.4. Interpolation and extrapolation of weld seam geometries

Furthermore, a statement to the type or direction of error is to be achieved. The training set consists of 20 instances, generated with numerical simulation, with constant process parameters for the metal sheet thicknesses of 1.5 mm and 2.0 mm. The trained MLP should then predict the material thickness of 1.7 mm (Fig. 8a). The MLP reaches a RMSE of 12.764 µm and shows a good qualitative and quantitative agreement with the curve. Fig. 8b shows the actual error between MLP prediction and test data for each examined joining time. It is noticeable that melting layer thicknesses are usually predicted to be too small, although the 1.7 mm are closer to the training data of 1.5 mm than to 2.0 mm.

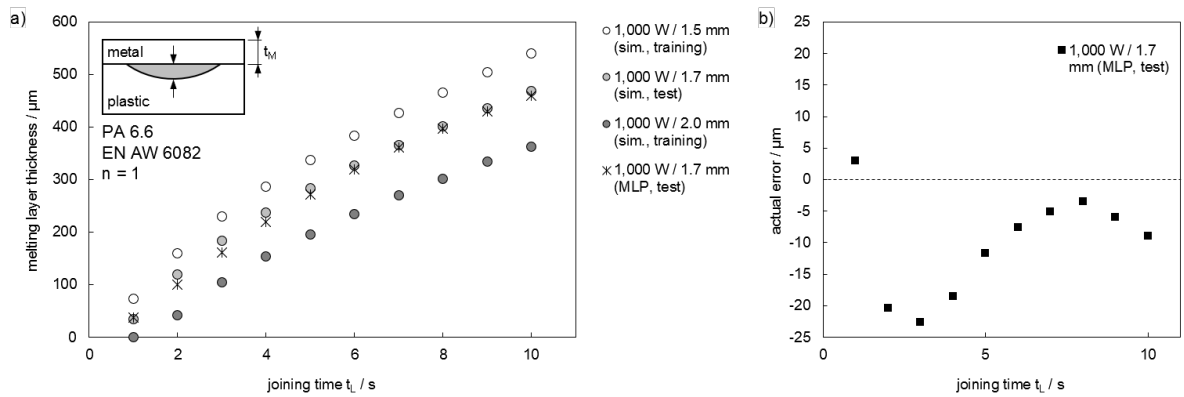

Fig. 8. Melting layer thickness for different metal sheet thicknesses and interpolation of an untrained sheet thickness (a); actual error of the MLP compared to the test data (b)

4. Conclusion

The aim of this paper is to demonstrate the capabilities of feed forward neural networks trained with back propagation as a powerful tool for the determination of the weld seam geometry in terms of melting layer thickness in laser-assisted joining of metal-plastic hybrids. Therefore, data sets based on experiments as well as numerical simulation are used. Support vector regression (SVR) is deployed as a method of comparison and the statistical parameters of mean absolute error (MAE), residual root mean square error (RMSE) as well as coefficient of determination (R^2) are applied to enable a quantitative evaluation of the training and validation process. The achieved results indicate excellent agreement between the training data and the predicted values which confirms an excellent performance of the used model. The application of such machine learning methods allows the generation of models which are able to accurately provide an appropriate prediction of geometrical welding parameters and has the potential to minimize the time and cost expense of further experimental or numerical investigations.

Acknowledgements

The authors would like to thank the Federal Ministry of Economic Affairs and Energy (BMWi) for the funding of the project “Mittelstand 4.0-Kompetenzzentrum Ilmenau” (funding reference: 01MF16005A).

References

Acherjee, B., Mondal, S., Tudu, B., Misra D., 2011. Application of artificial neural network for predicting weld quality in laser transmission welding of thermoplastics, Applied soft computing 11.2, p. 2548-2555.

Akbari, M, Saedodin, S., Panjehpour, A., Hassani, M., Afrand, M., Torkamany, M.J., 2016. Numerical simulation and designing artificial neural network for estimating melt pool geometry and temperature distribution in laser welding of Ti6Al4V alloy, Optik 127.23, p. 11161-11172.

Al-Sayyad, A.,Bardon, J., Hirchenhahn, P., Santos, K., Houssiau, L., Plapper, P., 2018. Aluminium Pretreatment by a Laser Ablation Process: Influence of Processing Parameters on the Joint Strength of Laser Welded Aluminum – Polyamide Assemblies, Procedia CIRP 74, p. 495-499.

Balasubramanian, K. R., Buvanashekaran, G., Sankaranarayanasamy, K., 2010. Modeling of laser beam welding of stainless steel sheet butt joint using neural networks, CIRP Journal of Manufacturing Science and Technology 3.1, p. 80-84.

Günther, J., Pilarski, P.M., Helfrich, G., Shen, H., Diepold, K., 2016. Intelligent laser welding through representation, prediction, and control learning: An architecture with deep neural networks and reinforcement learning, Mechatronics 34, p. 1-11.

Heckert, A., Zaeh, M., 2014. Laser Surface Pre-treatment of Aluminium for Hybrid Joints with Glass Fibre Reinforced Thermoplastics, Physics Procedia 56, p. 1171-1181.

Jacques, L., Abderrazak E. O., 2018 ANN based predictive modelling of weld shape and dimensions in laser welding of galvanized steel in butt joint configurations, Journal of Minerals and Materials Characterization and Engineering 6.03 p. 316-332.

Knaak, C., Thombansen, U., Abels, P., Kröger M., 2018. Machine learning as a comparative tool to determine the relevance of signal features in laser welding, Procedia CIRP 74, p. 623-627.

Liu, H., Qin, X., Huang, S., Jin, L., Wang, Y., Lei, K., 2018. Geometry characteristics prediction of single track cladding deposited by high power diode laser based on genetic algorithm and neural network, *International Journal of Precision Engineering and Manufacturing* 19.7,p. 1061-1070.

Mitchell, T. M., 2006. The Discipline of Machine Learning, Working paper, Carnegie Mellon University CMU-ML-06-10.

Nikolić, V., Milovančević, M., Petković, D., Jocić, D., Savić, M., 2018. Parameters forecasting of laser welding by the artificial intelligence techniques, Facta Universitatis, Series: Mechanical Engineering 16.2, p. 193-201.

Petković, D., 2017. Prediction of laser welding quality by computational intelligence approaches, Optik 140, p. 597-600.

Sathiya, P., Panneerselvam, K., Soundararajan, R., 2012. Optimal design for laser beam butt welding process parameter using artificial neural networks and genetic algorithm for super austenitic stainless steel, Optics & Laser Technology 44.6, p. 1905-1914.

Schricker, K., Bergmann, J. P., 2019. Temperature- and Time-Dependent Penetration of Surface Structures in Thermal Joining of Plastics to Metals, 22nd Symposium on Composites, accepted for publication, 8 p.

Schricker, K., 2018. Charakterisierung der Fügezone von laserbasiert gefügten Hybridverbunden aus teilkristallinen thermoplastischen Kunststoffen und Metallen, Schriften aus der Ilmenauer Fertigungstechnik 8, PhD thesis, Technische Universität Ilmenau.

Schricker, K., Stambke, M., Bergmann, J. P., 2015. Experimental investigations and modeling of the melting layer in polymer-metal hybrid structures, Welding in the World 59, p. 407-412.

Schricker, K., Bergmann, J. P., 2018. Determination of sensitivity and thermal efficiency in laser assisted metal-plastic joining by numerical simulation, Procedia CIRP 74, p. 511-517.

Stavridis, J., Papacharalampopoulos, A., Stavropoulos, P., 2018. A cognitive approach for quality assessment in laser welding, Procedia CIRP 72,p. 1542-1547.

Wasmer, K., Le-Quang, T., Meylan, B., Vakili-Farahani, F., Olbinado, M.P., Rack, A., Shevchik, S.A., 2018. Laser processing quality monitoring by combining acoustic emission and machine learning: a high-speed X-ray imaging approach, Procedia CIRP 74, p. 654-658.

Yuan, Bodi, et al., 2018. Machine-learning-based monitoring of laser powder bed fusion, *Advanced Materials Technologies* 3.12, 1800136.